

# Improved LIBS limit of detection of Be, Mg, Si, Mn, Fe and Cu in aluminum alloy samples using a portable Echelle spectrometer with ICCD camera

Walid Tawfik Y. Mohamed<sup>\*,1</sup>

*National Institute of Laser Enhanced Sciences NILES, Department of Environmental Applications, Cairo University, Cairo, Egypt*

Received 20 November 2006; received in revised form 9 March 2007; accepted 2 April 2007

Available online 9 May 2007

## Abstract

Laser-induced breakdown spectroscopy (LIBS) is a laser-based technique that can provide non-intrusive, qualitative and quantitative measurement of metals in various environments. LIBS uses the plasma generated by a high-energy laser beam to prepare and excite the sample in one step. In the present work, LIBS has been applied to perform elemental analysis of six trace elements simultaneously in aluminum alloy targets. The plasma is generated by focusing a pulsed Nd:YAG laser on the target in air at atmospheric pressure. LIBS limit of detection (LOD) is affected by many experimental parameters such as interferences, self-absorption, spectral overlap and matrix effect. We aimed to improve the LIBS LOD by optimizing these experimental parameters as possible. In doing so, a portable Echelle spectrometer with intensified CCD camera was used to detect the LIBS plasma emission. This advanced Echelle spectrometer provides a constant spectral resolution (CSR) of 7500 corresponding to 4 pixels FWHM over a wavelength range 200–1000 nm displayable in a single spectrum. Then, the calibration curves for iron, beryllium, magnesium, silicon, manganese and copper as minor elements were achieved with linear regression coefficients between 98–99% on average in aluminum standard sample alloys. New LOD values were achieved in the ppm range with high precision (RSD 3–8%). From the application view point, improving LIBS LOD is very important in the on-line industrial process control to follow-up multi-elements for the correct alloying in metals.

© 2007 Elsevier Ltd. All rights reserved.

*Keywords:* LIBS; Echelle spectrometers; Al alloys

## 1. Introduction

Laser-induced breakdown spectroscopy (LIBS), also known as laser-induced plasma spectroscopy (LIPS), offers unique capabilities for on-line composition determination. The use of LIBS as an analytical tool has considerably grown over the past 10 years. Spectrochemical analysis using LIBS has proven to be extremely versatile, providing multi-element analysis in real time without sample preparation. LIBS can be regarded as a universal sampling, atomization, excitation and ionization source, since laser-

induced plasmas can be produced in gases [1] or liquids [2], as well as from conducting or non-conducting solid samples [3,4].

In LIBS, a small volume of the target is intensely heated by the focused beam of a pulsed laser, and thus brought to a transient plasma state where the sample's components are essentially reduced to individual atoms. In this high-temperature plasma, atoms are ionized, or brought to excited states. Such states decay by emission of radiation, which is observed in the ultraviolet (UV), visible and near-infrared (NIR) regions of the spectrum. An atomic spectrum is obtained by means of a spectrograph, thereby allowing elemental components of the target to be identified and, using a calibration curve, quantified. LIBS measurements are generally carried out in ambient air at atmospheric pressure. For this reason, and also due to its rapidity, non-contact optical nature, and absence of sample

\*Fax: +9 664 642 4292.

E-mail address: [Walid\\_Tawfik@hotmail.com](mailto:Walid_Tawfik@hotmail.com).

<sup>1</sup>Present address: Education of Girls, Faculty of Education for girls, Department of Physics, Gurayat, North of Al-gouf, Kingdom of Saudi Arabia.

preparation, since the only requirement is the optical access to the samples, LIBS is a useful technique for on-line process analysis, which may thus satisfy the industrial requirements. The basic features of this spectroscopic technique and its applications for on-line measurements in industrial settings have been reviewed in several papers [1,5–8].

LIBS cannot be considered a non-destructive technique in the strictest sense, since a part of the target to be analyzed is vaporized and lost. However, the volumes sampled in this manner are very small:  $10^{-8}$ – $10^{-5}$  cm<sup>3</sup>, depending on the material, and the laser wavelength and fluence. Such volumes correspond to masses in the ng– $\mu$ g range. In the case of a solid sample, the lateral size of the laser-affected zone is typically less than 1 mm, and can be made as small as 1  $\mu$ m. In the vertical dimension, the thickness of material ablated by a laser pulse may, in the case of metals, be only tens of nanometers. When LIBS is applied to the analysis of fluids (e.g. water or molten metal), the issue of destructiveness is irrelevant, since the vaporized mass is negligible and the analyzed volume is continuously renewed.

LIBS measurements consist of spectral and time-resolved analysis of the atomic and ionic emission lines generated at the surface of a sample after focusing there an intense laser pulse [9–11]. Since the early application of LIBS for diagnostic purposes, several systems have been developed for both laboratory [12,13] and field use with portable units [14], taking advantage of its unique characteristics such as quickness, no sample preparation and very low sample consumption, and excellent depth profiling.

In the LIBS technique, the very high field intensity instantaneously evaporates a thin surface layer and initiates an avalanche ionization of the sample elements, giving rise to the so-called breakdown effect. LIBS spectra can be detected once the plasma continuum emission is almost extinguished. Time-resolved capability is necessary to discriminate the late atomic line emission from the early plasma continuum.

High-resolution spectral analysis is required to detect single emission lines, i.e. the spectral signatures of each element. The atomic and in some cases ionic lines, once assigned to specific transitions, allow for a qualitative identification of the species present in plasma. Their relative intensities can be used for the quantitative determination of the corresponding elements.

The method can be certified for analytical applications of material analysis in industry, assuming that the surface composition is maintained in the plasma and that the ablation process can be modeled in an appropriate temporal window with quasi-equilibrium conditions. Previous work [15] has demonstrated that several different experimental parameters (e.g. laser power and repetition rate, interaction geometry, surface conditions) may affect the effective analytical possibilities of the method, especially if a field application is foreseen which could make a profitable use of its main advantage of no sample pre-treatment needed.

On the other hand, for accurate quantitative analysis, three types of interferences—self-absorption, spectral overlap (spectral line interference, band interference), and matrix effect (chemical interferences)—have to be avoided in LIBS [16]. Self-absorption occurs when the emission from the hotter region absorbed by cool atoms is surrounded by the high-temperature core of the laser plasma. To avoid the problems with self-absorption, resonance lines should only be used for the measurement of trace elements. Spectral interference due to line overlap is very common, because the resolution depends upon the monochromator used. Care should be taken to avoid spectral interference lines in the analysis. Emission lines are often superimposed on bands emitted by oxides and other molecular species from air or samples. A background correction for band emission is necessary. The absolute intensity of an analyte line can be obtained by subtracting the peak height from the background signal near the analyte line. The physical and chemical properties of the sample can affect the plasma composition, a phenomenon known as the matrix effect. The matrix effect can result in the sample being ablated differently from the target sample. Previously published works studied the matrix effect under different experimental conditions to specify causes and find out the methods of correction [3,4,17–20].

In order to account for deviations in retrieved concentrations due to the matrix effect, a sophisticated modeling of the entire LIBS process, properly including plasma properties and thermal effects, is required for correcting the intensities of detected spectra lines. Barbini et al. [21] have shown that, especially in case of laboratory application, matrix effects can be minimized by using of internal standards by calibration with proper reference samples characterized by a similar matrix composition. In addition, plasma formation dynamics, sample ablation and associated processes are highly non-linear and not fully understood and may also play an important role as reasons of the matrix effect.

For analytical spectrochemistry by LIBS, the appropriate choice for the experimentalist is based on the combination of the spectrometer and the detector, which requires a compromise between wavelength coverage, spectral resolution, read time, dynamic range, and detection limit. The requirements for an ideal spectrometer–detector system to furnish simultaneous determination of any combination of elements in the spectrum include a high-resolution, wide spectral range, and high sensitivity and a linear response to radiation. Most of these requirements are in part fulfilled by a combination of Echelle spectrometer-intensified couple charged device ICCD detector. Recently, Echelle spectrometers were commercialized by three companies [22–24].

In the present work, we report the capability of a portable Echelle spectrometer–Mechelle 7500 equipped with ICCD camera to perform a high-precision quantitative analysis of Al alloys in air at atmospheric pressure. Many experimental parameters will be optimized to

improve the limits of detection of iron, magnesium, beryllium, silicon, manganese and copper in the aluminum alloys. In addition, the obtained results were compared with the previously obtained ones [3,25]. The purpose of this paper is to demonstrate the ability of the proposed compact setup to be used in real-time measurements in industrial applications in future.

## 2. Experimental setup

### 2.1. Instrumentation

A typical LIBS experimental setup, described in details by the author elsewhere [3,4] is used throughout the present investigations. The plasma formation was attained with the aid of a Q-switched Nd:YAG laser (surelite I, continuum, USA) operating at 1064 nm (pulse duration of 7 ns) and repetition rate of 0.1–10 Hz. An energy meter (Nova 978, Ophir Optronics Ltd., Wilmington MA 01887, USA) was employed to monitor the shot-to-shot pulse energy. The laser beam (about 5 mm diameter) with pulse energy of 300 mJ was focused on the aluminum alloy samples by a 10 cm focal length quartz lens to generate the plasma. A 1 m length fused-silica optical fiber mounted on a micro xyz-translation stage is used to collect the emission light from the plasma plume and feed it to a portable Echelle spectrometer of a 0.17 m focal length (Mechelle 7500, Multichannel instruments, Sweden). This fused-silica optical fiber, which is 600  $\mu\text{m}$  core diameter, 1 m length and numerical aperture of 0.22, is especially designed and calibrated for the Echelle spectrometer (Mechelle 7500) by Multichannel instruments, Sweden and the spectrometer has special plug-in port for this fiber (having a suitable coupling optics inside). The Echelle grating spectrometers designed for operation in high orders and high angles of incidence and diffraction, can provide high resolution in a more compact size and cover a much wider spectral range than conventional grating spectrometers [26]. The Mechelle 7500 provides a constant spectral resolution (CSR) of 7500 corresponding to 4 pixels FWHM over a wavelength range 200–1000 nm displayable in a single spectrum. A gateable, intensified CCD camera, (DiCAM-Pro-12 bit, UV enhanced, 43,000 channels, PCO Computer Optics, Germany) coupled to the spectrometer was used for detection of the dispersed light. The overall linear dispersion of the spectrometer camera system ranges from 0.006 (at 200 nm) to 0.033 nm/pixel (at 1000 nm). The usage of an intensified CCD camera has a great advantage on the SNR. Carranza et al. [27] recently compared non-intensified and intensified CCD detectors for LIBS. They concluded that the ICCD system yields a better performance for both ensemble-averaged and single-shot analyses, with improvements in SNR ranging from a factor of three to greater than one order of magnitude compared with CCD system. To avoid the electronic interference and jitters, the intensifier high voltage was triggered optically. Echelle spectra display,

control, processing and analysis were done using Mechelle software (Multichannel instruments, Stockholm, Sweden), GRAMS/32 version 5.1 Spectroscopic Data Analysis Software (Galactic Industries, Salem, NH, USA) and Origin software version 7.0220 (Origin Lab corporation, USA).

### 2.2. Optimization of data acquisition procedure

Many optimization procedures were performed to enhance the signal intensities of the trace elements and observing new detection limits. We have to keep in mind that in fact, minor changes in the experimental conditions may influence the detection limits. Here below, we optimized many experimental parameters to improve our LIBS resolution and sensitivity and to minimize the measurements fluctuations and problems due to the sample heterogeneity. These optimization procedures did not taken into consideration in our previous work [4].

Optimizing LIBS for a high-resolution aluminum alloy was done by optimizing the experimental conditions including the time delay, the gate delay (the integration time) and the laser irradiance. In fact, the timing of the recorded signal depends on the laser energy and wavelength, so we firstly increased the laser energy from 70 mJ, as used before by the author [4], to 300 mJ. In this case, the laser irradiance increased from  $\approx 10^8$ – $\approx 10^{10}$   $\text{W}/\text{cm}^2$ , which found to be suitable for the case of aluminum alloy samples having trace elements with concentrations in the ppm range. Then under the late laser irradiance, the delay time, at which the spectrum is recorded from the laser start, was optimized by scanning the delay time with the signal intensity as done previously by the author [4]. It was found that the optimized conditions are 2.5  $\mu\text{s}$  delay time and 1.5  $\mu\text{s}$  gate width at  $10^{10}$   $\text{W}/\text{cm}^2$  laser irradiance at the sample surface. The gate delay was limited to 1.5  $\mu\text{s}$  to avoid saturation of the detector. Optimizing LIBS spectrum was done in order to reduce the background signal and increase the SNR (see the following Section 3.1). This, of course, makes LIBS to be a high resolution and a high sensitive spectroscopic system for the trace elements with concentrations in the ppm range, which returns improvements in the detection limits of the system.

Moreover, the Mechelle spectrometer needs internal calibration from time to time. Due to variations in laboratory temperature, the spectrum shifts approximately 5–25 pixels on a day-to-day basis, if uncalibrated. To avoid this problem, the spectrometer is wavelength calibrated using a mercury lamp source (Hg lines at 253.65, 435.83, 546.07 nm). This procedure, which was not taken into consideration before, improves the resolution to be 0.045 nm, which is about five times higher than observed before (0.2 nm) [3,4]. Moreover, pre-exposure was performed to set the response of the CCD so the camera would not oversaturate.

To improve data reproducibility, and to avoid electronic jittering problem, the laser was set to single shot mode.

Then, the Nd:YAG laser beam was focused onto the sample surface at 90° angle. This was done using a 25 mm diameter fused-silica dichroic mirror (continuum, USA) that reflects 99% of high energy 1064 nm wavelength. The focal point was set 5 mm below the surface of the sample in order to generate plasma of 800 μm spot diameter. This also minimizes breakdown above the surface of any particles and aerosols generally present above the sample. On the other hand, the use of a micro xyz-translation stage as a holder for fused-silica optical fiber facilities maximum intensity of the observed emission light from the plasma plume. We investigated a set of eight standard samples of aluminum alloy to establish calibration curves for six elements Be, Mg, Si, Mn, Fe and Cu by the proposed LIBS setup. These samples have never been treated before using LIBS with Mechelle 7500 and, were selected, so that the trace elements concentrations were about ten times lower than samples used in previous work [3,4]. It is found that low trace elemental concentrations increase the measurements sensitivity [16]. This is because, at high analyte concentrations, a loss of measurements sensitivity occurred due to self-absorption in the laser plume. We used disk shaped standard samples of aluminum alloy provided by Alcan international limited (0.5 cm;  $\phi = 5$  cm). The concentrations of Mg, Si, Be, Cu, Mn and Fe in the aluminum alloy samples are given in Table 1.

For each new sample, before spectral collection, 20 laser pulses were performed to clean the sample surface and remove surface oxides and contamination to ensure that the observed spectrum is representative of the sample composition.

Now, we aim to produce LIBS spectra with high precision. Precision is the measure of the degree of reproducibility of a measurement. It is generally measured as the RSD of a set of repeated measurements precision. Typical LIBS precision is 5–20% [16]. Laser shot-to-shot variation causes differences in the plasma properties, therefore affects the magnitude of the element signal, and hence degrades the LIBS precision. To improve LIBS precision, spectra from several laser shots have to be averaged in order to reduce statistical error due to laser shot-to-shot fluctuation. Moreover, we found that enhancement of the data reproducibility can be achieved by

accumulation of consecutive measured spectra. We reproduced the measurements at five locations on the sample surface in order to avoid problems linked to sample heterogeneity. Twenty shots were fired at each location and saved in separated files and the average was computed and saved to serve as the library spectrum. Moreover, for each spectrum recorded, the peak intensity, the full-width half at maximum (FWHM), and the center wavelength of each line, as well as the background emission continuum were determined. Data treatment preprocessing of the averaged spectra data was performed in the Windows environment on a Pentium III PC using GRAMS/32 version 5.2 (Thermo Galactic, USA.) and Excel (Microsoft office Excel 2003). The averages of peak tables (lists of wavelengths and intensities) of the averaged spectra were roll generated in GRAMS/32 and exported for data evaluation.

### 3. Results and discussion

#### 3.1. Qualitative analysis

One of the most promising approaches to atomic emission spectroscopy (AES) and particularly for the LIBS experiment involves the use of a portable Echelle spectrometer [12,28–30]. Hence, for industrial applications, it is necessary to be able to analyze several elements at once; therefore, the use of an Echelle spectrometer that covers the emission spectra from the UV to visible with sufficient resolution is desirable.

Hundred laser shots were accumulated on the ICCD of the system to analyze each sample. The spectrum can be investigated simultaneously with an Echelle spectrometer (typically 200–700 nm); the wavelengths of interest (with minimum around 251 nm for Si and maximum around 518 nm for Mg) in several spectral windows are presented. The optimized experimental parameters for laser pulse energy, gate delay time, gate width, number of accumulated single shot spectra, and geometrical arrangements are fixed for all experimental data acquisition procedures.

Fig. 1 shows a typical plasma emission spectrum for aluminum alloy sample Al 5754. This spectrum is the average of 100 single shot spectra recorded at 2.5 μs delay time and 1.5 μs gate width. The panoramic Echelle spectra in the spectral range 200–700 nm show the UV–visible emission lines of aluminum as a major element and the emission lines of Si, Cu, Be, Fe, Mn and Mg as trace elements in the aluminum alloy sample.

Fig. 2 shows zoomed windows in the UV range 278–313 nm of the total spectrum of aluminum alloys. These spectra show narrow and intense analytical atomic lines appeared even in trace levels of elemental concentrations in an aluminum alloy sample. Fig. 2a shows a spectrum of four elements where the emission lines starting with two lines for Mg at 279.55, 280.27 nm, then four lines, Al line at 281.62 nm, Mg line at 285.21 nm, Si line at

Table 1  
Beryllium, copper, iron, magnesium, silicon and manganese concentrations (in w/w%) in the standard aluminum alloy samples

Sample	Be	Mg	Si	Fe	Cu	Mn	Al
AL 3104	0.0011	1.15	0.21	0.42	0.17	0.92	Balance
AL 4104	0.0017	1.56	9.63	0.7	0.12	0.046	Balance
AL 5052	0.0043	2.51	0.087	0.33	0.042	0.09	Balance
AL 5182	0.0012	4.67	0.11	0.27	0.061	0.35	Balance
AL 5754	0.0022	2.54	0.22	0.35	0.1	0.29	Balance
AL 6063	0.00030	0.54	0.43	0.2	0.085	0.081	Balance
AL 7010	0.0007	2.44	0.11	0.22	1.88	0.082	Balance
AL a380.2	0.00036	0.028	9.17	0.41	3.61	0.042	Balance

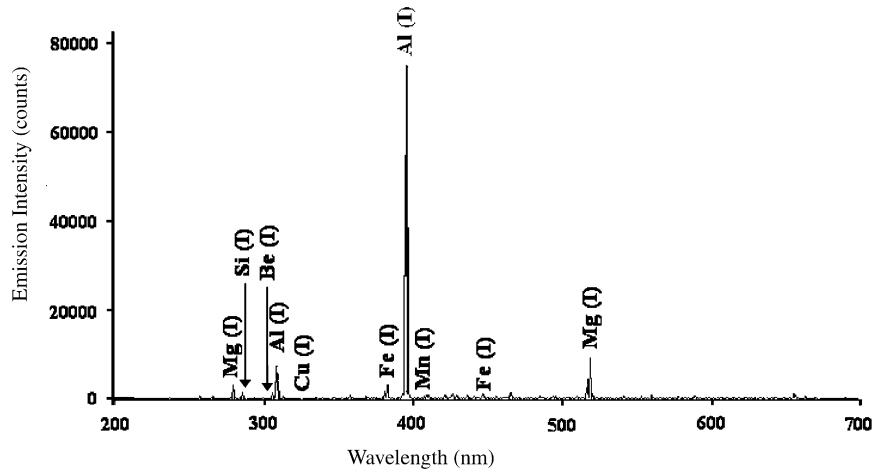


Fig. 1. Typical LIBS spectrum for aluminum alloy target. The laser energy was 300 mJ at wavelength 1064 nm and the plasma emissions were accumulated with delay 2.5  $\mu$ s, and gate width 1.5  $\mu$ s.

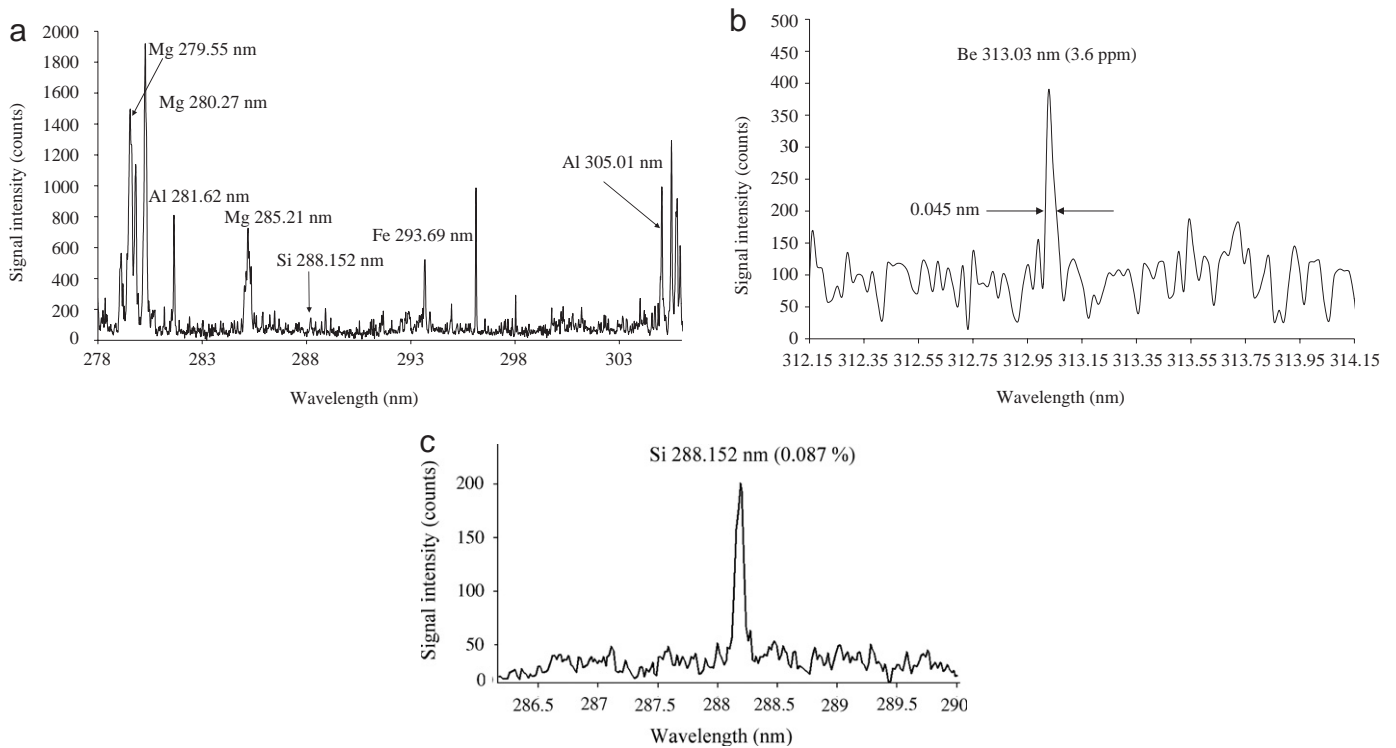


Fig. 2. Several windows in the UV range for elements in aluminum alloys. (a) Shows a spectrum of four elements Mg, Al, Fe and Si. (b) Shows a high resolution spectrum of beryllium line at 313.03 nm with resolution 0.045 nm ( $\lambda/\Delta\lambda = 6956$ ) and SNR = 2.56 for concentration of 3.6 ppm in aluminum alloy sample Al a380.2. (c) Shows a spectrum of aluminum alloy sample Al 5052 for silicon at line 288.152 nm of 0.087% concentration with resolution 0.075 nm ( $\lambda/\Delta\lambda = 3842$ ) and SNR = 8.

288.152 nm and Fe line at 293.69 nm and ending with the well resolved aluminum atomic line at 305.01 nm. Fig. 2b shows a high-resolution spectrum of beryllium line at 313.03 nm with resolution 0.045 nm ( $\lambda/\Delta\lambda = 6956$ ) and SNR = 2.56. These measurements were done on aluminum alloy sample Al a380.2 with Be concentration of 3.6 ppm.

Fig. 2(c) shows a spectrum of aluminum alloy sample Al 5052 for silicon at line 288.152 nm of 0.087% concentration with resolution 0.075 nm ( $\lambda/\Delta\lambda = 3842$ ) and SNR = 8. The observed results revealed that, by increasing the trace

content concentration, SNR may enhance but with losing some spectral resolution, i.e.  $\lambda/\Delta\lambda$  decreases, which in agreement with Fang-Yu Yueh et al. [16]. Moreover, the obtained spectra are great better than observed before by Mohamad Sabsabi et al. [3]. They observed the beryllium line at 313.03 nm with resolution 0.2 nm and SNR = 2 for concentration 13 ppm in aluminum alloy sample.

Moreover, our observed spectra reflect the wide spectral range and the high resolution of the used spectroscopic system. These improve both the reliability and

reproducibility of the used LIBS technique that was needed for the quantitative analysis of the aluminum alloy samples.

### 3.2. Quantitative analysis and calibration curves

Based on our qualitative investigation of the aluminum alloy samples by LIBS, we are now in a position to determine the most suitable conditions for the quantitative analysis of these aluminum alloys. Here below, we tried to avoid the experimental fluctuations and all types of interferences to observe calibration curves for the trace elements with good linearity and lower detection limits than obtained before [4].

Standardization method has been exploited to avoid any unwanted experimental fluctuations [31]. The ratio of the line intensity of trace element to the emission line of the internal standard is measured and plotted as a function of the known concentration ratios of the reference samples. The proper emission line of the internal standard has been chosen by comparing different calibration curves of the same element obtained using different internal standards and different emission lines. The element and line giving the best linear relation (the highest value of the correlation coefficient  $R$ ) are chosen as internal standards. The performed optimization in case of the minor elements in the aluminum alloy revealed that the best internal standard is the Al atomic line at 305 nm. This is in agreement with previously published data, recommending the use of a major element in the matrix as an internal standard [4,25].

To avoid self-absorption and spectral line interference, three rules were used for the selection of the appropriate wavelength for each element. First rule, we have to avoid interference between spectral lines for different species. So that, interfering lines like Fe (281.7 nm) and Al (281.61 nm), and Fe (285.3 nm) and Mg (285.29 nm), and similar lines were avoided. Second rule, avoiding the possibility of self-absorption in the case of lines ending in a heavily populated level, such as resonant lines. So that lines like Al (394.5 nm), Al (396.26), Al (308.30 nm), Al (309.36 nm), Fe (271.9 nm), Si (251.50 nm), Mg (280.27 nm) and Mg (279.55 nm) were avoided.

Third rule, to perform a matrix-independent measurement, beside the internal standardization, the elements

must have approximately the same excitation energies [16]. Table 2 lists the selected elemental wavelengths and their corresponding excitation energies. Except for silicon excitation energy, most of the selected elemental wavelengths have excitation energies little lower or closer to the Al 305 nm excitation energy. This means that silicon needs more energy to be excited. So, we expect that silicon will have higher detection limits than the rest of the trace elements.

The wavelengths of the spectral lines used throughout the analysis were Mg (518.36 nm), Si (288.15 nm), Mn (403.07 nm), Be (313.05 nm), Fe (404.53 nm) and Cu (324.75 nm). With time-resolved spectroscopy, the emission signal becomes very low and not all the lines are detected specially for trace elements. So that, we were enforced to use resonance lines for Mn, Be and Cu. Normally, we have to avoid such lines in the quantitative analysis since they are subjective of high self-absorption as described above. Since the number density of the atomic species of Be, Mn, and Cu in the plasma plume is low due to their low concentration in the target material, self absorption effect may be neglected within the experimental uncertainty. So, these lines are good candidates for a lower limit of detection (LOD) due to its strength compared with other atomic emission lines. In fact, this is in agreement with the observations of Drogoff et al. [25], and Sabsabi et al. [3].

The emission intensities of each element were normalized to the emission intensity of Al atomic line at 305 nm to reduce both the effect of instrument signal fluctuation and the matrix interference effects. The calibration curves of the studied elements were obtained by drawing the normalized intensities against their relative concentrations. The corresponding normalized calibration curves are given in Fig. 3 for aluminum alloy samples. Each data point represents the mean value of typically five individual measurements. The given error bars show the calculated standard deviation for the measured LIBS intensities for each trace content of the aluminum alloy sample. They represent the variation in our measurements.

Calibration curves of the elements in the aluminum matrix pass nearly through the origin and have well linear fitting ( $R^2 > 0.9$ ) within the experimental uncertainty. The obtained linear equations and  $R^2$  values for each element are listed in Table 2. The observed linear calibration equations and the correlation coefficients  $R^2$  indicate good linearity within two orders of magnitude. In fact, this result gives an expectation that the proposed LIBS technique has a capability for a good linearity of the calibration curves attaining a wide range of elemental concentrations.

The LOD was calculated from the formula [32]

$$\text{LOD} = 3\sigma/s,$$

where  $\sigma$  is the standard deviation of the background and  $s$  is the calibration slope. The obtained LOD values and their relative standard deviation (RSD %), for Mg, Si, Mn, Fe, Be and Cu are listed with the previously obtained values [3,25] in Table 3. It is clear that we have new LOD values

Table 2  
Spectroscopic data of prominent analyte and reference lines used for LIBS analysis of aluminum alloys

Element	Wavelength (nm)	$E_i$ (eV)	$E_k$ (eV)	$\Delta E$ (eV)
Al	305.00	3.60384	7.66762	4.06378
Fe	404.58	1.48486	4.54851	3.06364
Cu	324.75	0	3.81673	3.81673
Be	313.04	0	3.95948	3.95948
Si	288.15	0.78096	5.08235	4.30139
Mg	518.36	2.71664	5.10783	2.39119
Mn	403.07	0	3.07509	3.07509

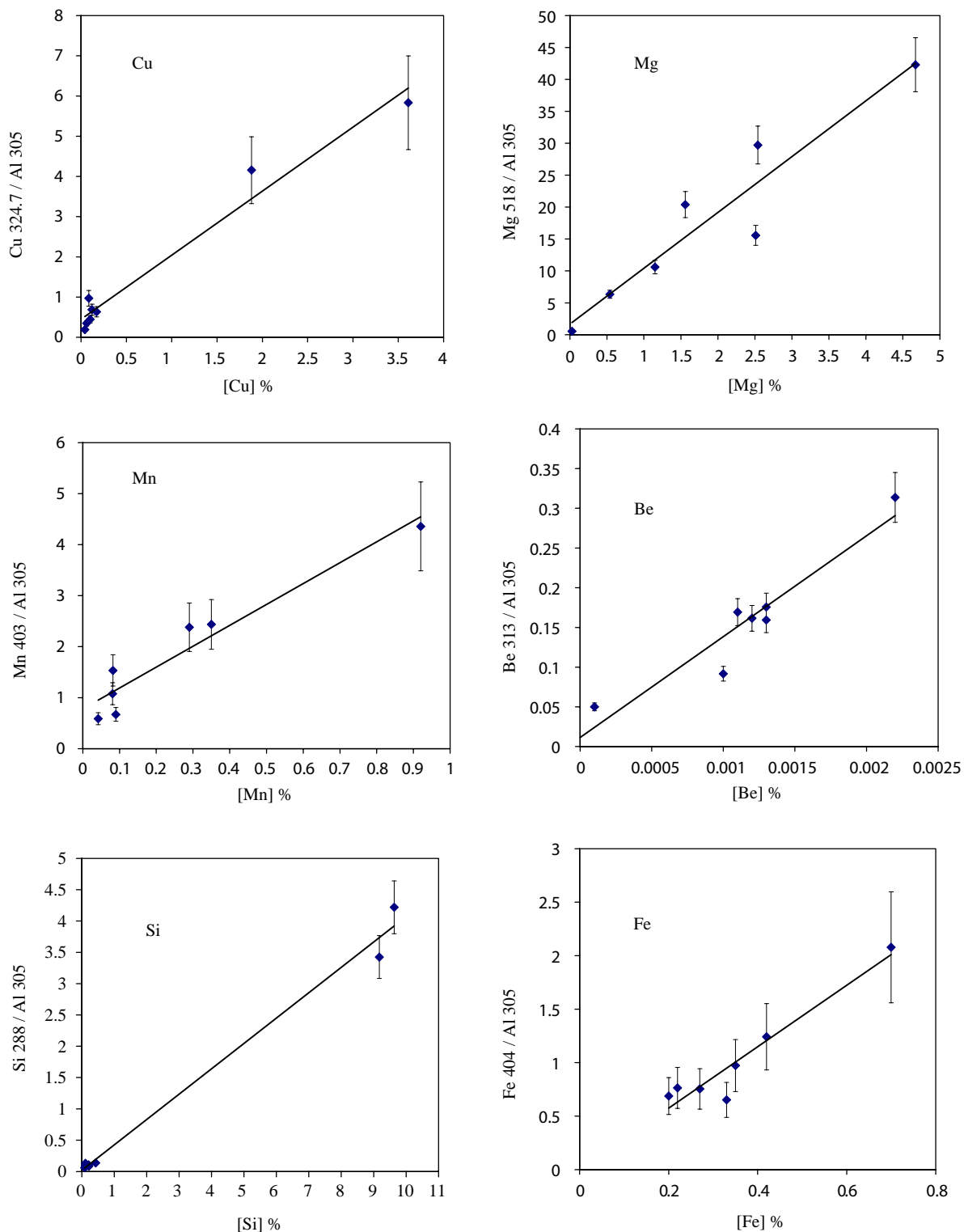


Fig. 3. Calibration curves for Cu, Mg, Mn, Be, Si and Fe in aluminum alloy. The calibration curves of the studied elements obtained by drawing the normalized intensities against their relative concentrations. Each data point represents the mean value of typically five individual measurements. The given error bars show the calculated standard deviation for the measured LIBS intensities for each trace content of the aluminum alloy sample. All elements were performed at  $2.5\ \mu\text{s}$  delay time and  $1.5\ \mu\text{s}$  gate time using 300 mJ Nd:YAG laser operating at 1064 nm and 7 ns pulse duration.

with a high precision (RSD 3–8%). Silicon has slightly high LOD in aluminum matrix. This observation can be explained considering the excitation energy for silicon

transition state ( $3s^2 3p^2-3s^2 3p 4s$ ) at 288.15 nm which is higher than that of Al at 305 nm ( $3s 3p^2-3s 3p 4s$ ), as shown in Table 2, this may have some effect on the

Table 3

Limit of detection (LOD), relative standard deviation (RSD%), correlation coefficient ( $R^2$ ) values, and calibration equation for the elements under study in the aluminum alloy samples

Element	Wavelength of the spectral line used (nm)	LOD values (ppm) Present work	LOD values (ppm) Previous work	RSD%	$R^2$	Calibration equation
Be	313.05	0.22	0.4 [3]	8.22	0.9015	$y = 127.05x + 0.0113$
Mg	518.36	3.19	5.5 [3]	3.35	0.8965	$y = 8.7427x + 1.6886$
Si	288.152	68.74	136 [3]	8.74	0.9908	$y = 0.4051x + 0.0207$
Mn	403	6.81	18 [3]	4.94	0.9252	$y = 4.0952x + 0.7778$
Cu	324.75	17.49	30.4 [3]	5.59	0.9691	$y = 1.5924x + 0.4500$
Fe	404.58	9.71	84.5 [25]	8.23	0.9193	$y = 2.8691x + 0.0011$

obtained values of the LOD of the studied elements in Al matrix mainly due to the ease of the energy transfer between the elements within matrix.

Under our new optimized conditions, all the obtained LOD values are improved by more than 50% of the previously observed values by the author [3] for all elements, except iron. For iron, no previous LOD values found for Fe in aluminum alloys using Echelle spectrometer. So that, we compared our Fe LOD value with the results of Drogoff et al. [25]. They worked on the same standard aluminum alloy samples using a sophisticated LIBS setup containing femtosecond laser Ti:sapphire laser 800 nm, with a pulse duration of 100 fs and power density is  $0.2 \text{ TW/cm}^2$  and a 50-cm Czerny-Turner spectrometer with ICCD camera. Even using this huge system, they obtained LOD for Fe at 404.5 nm with value 84 ppm. In our case, while we used simpler system, we obtained LOD for Fe at 404.5 nm with value 9.71 ppm.

#### 4. Conclusion

In summary, we have carried out an accurate LIBS setup using the advanced portable Echelle spectrometer (Mechelle 7500) equipped with ICCD detector for qualitative and quantitative analysis of six trace elements in Al alloy samples simultaneously. The Mechelle 7500 provides a wide spectral range with high resolution that facilitates LIBS to detect elements with more accuracy and high sensitivity. Moreover, the obtained results showed that by optimizing the experimental parameters and carefully selecting appropriate wavelength for each trace element, the detection limits could be improved. The observed limits of detection for Be, Mg, Si, Mn, Fe and Cu are better than the values published by previous groups. Moreover, the proposed LIBS setup is compact and could be transported. In future, this system could be arranged in one cabinet with dimensions  $80 \times 80 \times 100 \text{ cm}$  since the Mechelle spectrometer including the ICCD camera is 30 cm long, 14 cm wide and 17 cm high and the Nd:YAG laser (surelite I) is about 60 cm in length, 15 cm in width and 15 cm in height. All of these facilitate it to be used for in situ real-time industrial process control and follow-up multi-elements for the correct alloying in metals.

#### Acknowledgments

The author gratefully acknowledges the support of Prof. Mohamed Abel-Harith and Prof. M. Sabsabi specially for offering the aluminum alloy samples.

#### References

- [1] Radziemski LJ. Review of selected analytical applications of laser plasmas and laser ablation, 1987–1994. *Microchem J* 1994;50:218–34.
- [2] Mohamed WTY. Quantitative elemental analysis of seawater by laser induced breakdown spectroscopy. *Int J Pure Appl Phys* 2006;2(1): 11–21.
- [3] Sabsabi M, Detalle V, Harith MA, Tawfik W, Imam H. Comparative study of two new commercial Echelle spectrometers equipped with intensified CCD for analysis of laser-induced breakdown spectroscopy. *Appl Opt* 2003;42(30):6094–8.
- [4] Ismail MA, Imam H, Elhassan A, Youniss WT, Harith MA. LIBS limit of detection and plasma parameters of some elements in two different metallic matrices. *J Anal At Spectrom* 2004;19:489–94.
- [5] Rusak DA, Castle BC, Smith BW, Winefordner JD. Fundamentals and applications of laser-induced breakdown spectroscopy. *Crit Rev Anal Chem* 1997;27:257–90.
- [6] Sneddon J, Lee Y-I. Novel and recent applications of elemental determination by laser-induced breakdown spectrometry. *Anal Lett* 1999;32:2143–62.
- [7] Tognoni E, Palleschi V, Corsi M, Cristoforetti G. Quantitative micro-analysis by laser-induced breakdown spectroscopy: a review of the experimental approaches. *Spectrochim Acta B* 2002;57:1115–30.
- [8] Majidi V, Joseph MR. Spectroscopic applications of laser-induced plasmas. *Crit Rev Anal Chem* 1992;23:143–62.
- [9] Ciucci A, Palleschi V, Rastelli S, Barbini R, Colao F, Fantoni R, et al. Trace pollutants analyses in soil by a time-resolved laser induced breakdown spectroscopy technique. *Appl Phys B* 1996;63:185–90.
- [10] Ciucci A, Corsi M, Palleschi V, Rastelli S, Salvetti A, Tognoni E. A new procedure for quantitative elemental analyses by laser induced plasma spectroscopy. *Appl Spectrosc* 1999;53:960–4.
- [11] Piepmeyer EH. Laser ablation for atomic spectroscopy, analytical application of laser. New York: Wiley; 1986.
- [12] Bauer HE, Leis F, Niemax K. Laser induced breakdown spectrometry with an echelle spectrometer and intensified charge coupled device detection. *Spectrochim Acta Part B* 1998;53:1815–25.
- [13] Russo RE, Mao XL. Chemical analysis by laser ablation. In: Miller JC, Haglund RF, editors. *Laser Experimental Ablation and Desorption*. San Diego: Academic Press; 1998. p. 375.
- [14] Yamamoto KY, Cremers DA, Ferris MJ, Foster LE. Detection of metals in the environment using a portable laser-induced breakdown spectroscopy instrument. *Appl Spectrosc* 1996;50:222–33.
- [15] Castle BC, Talabardon K, Smith BW, Winefordner JD. Variables influencing the precision of laser-induced breakdown spectroscopy measurements. *Appl Spectrosc* 1998;52:649–57.



- [16] Yueh Fang-Yu, Singh JP, Zhang H. Laser-induced Breakdown Spectroscopy: Elemental Analysis. In: Meyers RA, editor. Encyclopedia of Analytical Chemistry. Chichester: Wiley; 2000. p. 2066–87.
- [17] Bulatov V, Krasniker R, Schechter I. Study of matrix effects in laser plasma spectroscopy by combined multifiber spatial and temporal resolutions. *Anal Chem* 1998;70:5302–10.
- [18] Xu L, Bulatov V, Gridin V, Schechter I. Absolute analysis of particulate materials by laser-induced breakdown spectroscopy. *Anal Chem* 1997;69:2103–8.
- [19] Goode SR, Morgan SL, Hoskins R, Oxsher A. Identifying alloys by laser-induced breakdown spectroscopy with a time-resolved high resolution echelle spectrometer. *J Anal At Spectrom* 2000;15:1133–8.
- [20] Eppler AS, Cremers DA, Hickmott DD, Ferris MJ, Koskelo AC. Matrix effects in the detection of Pb and Ba in soils using laser-induced breakdown spectroscopy. *Appl Spectrosc* 1996;50:1175–81.
- [21] Barbini R, Colao F, Fantoni R, Pallucci A, Ribezzo S. Semi-quantitative time-resolved LIBS measurements. *Appl Phys B* 1997;65:101–7.
- [22] Multichannel Instruments AB, Sweden.
- [23] Catalina Scientific Corporation, USA <<http://www.catalinasci.com/se200.cfm>>.
- [24] LLA Instruments GmbH, Germany <<http://www.lla.de/en/index.php/content/view/13/40/>>.
- [25] Le Drogoff B, Margotb J, Chakera M, Sabsabi M, Barthelemy O, Johnstona TW, et al. Temporal characterization of femtosecond laser pulses induced plasma for Spectrochemical analysis of aluminum alloys. *Spectrochimica Acta Part B* 2001;56:987–1002.
- [26] Olesik JW. Echelle grating spectrometers for inductively coupled plasma-optical emission spectrometry. *Spectroscopy* 1999;14(10):27–30.
- [27] Carranza JE, Gibb E, Smith BW, Hahn DW, Winefordner JD. Comparison of nonintensified and intensified CCD detectors for laser-induced breakdown spectroscopy. *Appl Opt* 2003;42(30):6016–21.
- [28] Becker-Ross H, Florek SV. Echelle spectrometers and charge-coupled devices. *Spectrochim Acta Part B* 1997;52:1367–75.
- [29] Haisch C, Panne U, Niessner R. Combination of an intensified charge coupled device with an echelle spectrograph for analysis of colloidal material by laser-induced plasma spectroscopy. *Spectrochim Acta Part B* 1998;53:1657–67.
- [30] Lindblom P. New compact Echelle spectrographs with multichannel time-resolved recording capabilities. *Anal Chim Acta* 1999;380:353–61.
- [31] Yoon Y, Kim T, Yang M, Lee K, Lee G. Quantitative analyses of pottery glaze by laser induced breakdown spectroscopy. *Microchem J* 2001;68:251–6.
- [32] Ingle JD, Crouch SR, Lafferty KM, editors. *Spectrochemical Analysis*. New Jersey, USA: Prentice Hall; 1988.